The Pennsylvania State University

College of Earth and Mineral Sciences

# QUANTIFYING VEGETATION COVER AND ECOSYSTEM SERVICES WITH HYPERSPATIAL UAS IMAGERY IN A COASTAL INTERMEDIATE MARSH

A Capstone Summary in

Geography

by

Whitney P. Broussard III

Submitted in Partial Fulfillment
of the Requirements
for the Degree of

Master of Geographic Information Systems

August 2017

## ABSTRACT

$15-20 billion is projected to be spent on restoration projects in the next several decades along the northern Gulf Coast. There is a need for efficient monitoring procedures that capture information from this endeavor on both the landscape scale and the local scale. Recent developments in Unmanned Aircraft Systems (UAS) have sparked interest in the ability of these systems to capture remotely sensed data to meet monitoring needs in coastal wetlands. This research demonstrates the ability of UAS technology to collect hyperspatial, multispectral aerial images and produce 2-dimensional orthomosaics and 2.5-dimensional digital surface models in a *Spartina patens* dominated intermediate coastal marsh. Object-Based Image Analysis techniques were used to classify species composition and quantify average plant height, land-water interface, and Normalized Difference Vegetation Index (NDVI). Model results were validated with on-the-ground CRMS vegetation surveys. A case study of CRMS station 0392 in Terrebonne Parish is presented, including results of the spatial analysis and some logistical constraints and lessons learned from operating a UAS in the coastal environment. These methods can be readily applied in multiple coastal settings of different habitat types, and can support other project operations and monitoring needs. Widespread deployment of such a method would be an important step towards a comprehensive monitoring program of coastal restoration and would provide a useful tool to study how coastal wetland ecosystems respond and adapt to human interventions.

## ACKNOWLEDGEMENTS

I would like to thank the University of Louisiana at Lafayette and the Institute for Coastal and Water Research for support and funding throughout this endeavor. Special thanks to Ed Theriot for the funding allocation and to Grant Kleiner for his help in the field. JESCO Environmental and Geotechnical Services, Inc. is the owner and operator of the UAS that was used in this project, and the instigator of my decision to pursue this line of research. They have been a champion of my work and supported my fieldwork both financially and logistically. Special thanks to Tom Cousté, Alvinette Teal, Shayne Teal, and Ben Landy of JESCO for their friendship and help in the field. Thank you to my Penn State Department of Geography capstone advisor Rob Brooks for his guidance and support, especially helping me to the link GIS and remote sensing with ecology. Thanks to Qassim Abdullah for his instruction on the use and application of UAS technology. Thanks to Jarlath O'Neil-Dunne who taught me object-based image analysis. Thank you as well to Leigh Anne Sharp with the Coastal Protection and Restoration Authority and to Sarai Piazza with the U.S. Geological Survey. Early in the process, they helped me develop the core ideas and research questions from a practitioner's perspective. And thank you to my long-time friend and mentor Jenneke Visser who has supported me as a post-doctoral advisor, a director, a colleague, and a friend. I genuinely appreciate her knowledge of wetland plants and her passion for coastal Louisiana, and I am the better for having spent these last 9 years working under her guidance. Finally, I am grateful to my wife and two daughters who allowed me the time on nights and weekends to pursue this degree. It takes a whole family to complete a challenge like this and I could not have done it without them.

# TABLE OF CONTENTS

## I. Background and Rationale

Louisiana's coastal wetlands account for roughly 22% of the total coastal wetland area of the lower 48 conterminous United States (Gosselink, 1984) and provide protection for infrastructure that supplies 90% of the nation's outer continental oil and gas, 20% of the nation's annual waterborne commerce, 26% (by weight) of the continental U.S. commercial fisheries landings, winter habitat for five million migratory waterfowl (Coastal Protection and Restoration Authority of Louisiana 2012) The land loss crisis in coastal Louisiana has claimed 4,833 square kilometers of land from 1932 to 2016 (Couvillion et al. 2016) with the potential to lose up to an additional 1,750 square miles of land (Coastal Protection and Restoration Authority of Louisiana 2012)

Land loss in Louisiana is driven by both natural and human factors. Levees and floodgates on the Mississippi River have deprived the coastal ecosystem of the fresh water and sediment it needs to survive (Day et al. 2000). Dredging canals for oil and gas exploration and pipelines distrupts natural hydrology, weakens marshes, and allows salt water to move inland (Turner 1997). Deepwater Horizon oil spill and other environmental impacts have directly and indirectly impacted Louisiana's coast (Baker, Steinhoff, and Fricano 2016).

These landscapes are important for various reasons. They are naturally occurring and therefore afforded due respect simply because they exist. From an anthropogenic perspective, wetlands offer valuable ecosystem services (Costanza et al. 1997; Brooks et al. 2007). Many of the proxies for valuing ecosystem services involve evaluating the quality and quantity of habitat to support various fish and wildlife (Freeman III 1991; Bell 1997). Coastal wetlands reduce the effects of storm surge and waves on coastal communities. Storm surge reduction models are often based on the location and amount of land in proximity to population centers, type of vegetation, and land elevation (Costanza et al. 2008). The Wetland Morphology Model of the Louisiana Master Plan for a Sustainable Coast was used to estimate project effects on carbon storage potential (Coastal Protection and Restoration Authority of Louisiana 2012). Carbon storage in wetlands is considerable, plays a role in global carbon budgets, and varies with the type of wetland, the acreage, and the annual vertical accretion of soil, and aboveground biomass (Mitsch and Gosselink 2007; Barbier et al. 2011). Nutrient uptake and removal in both sediments and wetland plants is beneficial (Craft 2007; Craft et al. 2009).

## II. Introduction to Research Problem

*Coastal wetlands monitoring*

Current monitoring programs for coastal vegetation in Louisiana include two main components: a coastwide helicopter survey and the Coastwide Reference Monitoring System. Coast-wide Reference Monitoring System (CRMS) stations are located throughout the Louisiana coastal zone and serve as the ambient coastal wetland monitoring network for the region (Steyer 2010). These CRMS stations have 200m x 200m on-the-ground sampling locations for species cover, plant height, and land water interface, and will be used as a reference dataset for this project. Additionally, the State of Louisiana and US Geological Survey use coast-wide helicopter surveys along north-south transects spaced 3 km apart with sampling sites located at 0.8 km along the transects to monitor large-scale changes in wetland vegetation (Sasser et al. 2014). While hovering over a sampling site, ocular estimates are used to record the dominant species present and to determine the percent of total cover for each species using a Braun-Blanquet cover scale (R = singular, Plus = <1, 1 = 2-5%, 2 = 6-25%, 3 = 26-50%, 4 = 51-75%, 5 = 76-100%). These surveys are costly and are currently reproduced once every 7 years.

Traditional remote sensing techniques have been used to develop vegetation maps by species, biomass estimates, and marsh health indicators (NDVI etc.). The Ramsar Convention on Wetlands supports the development and application of remote sensing and GIS to fill gaps in baseline wetland inventories

(Rebelo, Finlayson, and Nagabhatla 2009). European Remote Sensing (ERS) satellite radar data has been used to estimate biomass information (Moreau and Le Toan 2003). Hyperspectral image analyses have mapped salt-marsh vegetation (Belluco et al. 2006) and identify invasive vegetation in a wetland deltaic ecosystem (Hestir et al. 2008). Gilmore et al. (2008) examined the effectiveness of using multi-temporal satellite imagery, field spectral data, and LiDAR (Light Distance and Ranging) top-of-canopy data to classify and map the common plant communities of the Ragged Rock Creek marsh, located near the mouth of the Connecticut River. Multispectral image processing has identified vegetation species in rangeland environments (Laliberte and Rango 2011). Couvillion et al. (2011) used historical surveys, aerial data, and satellite data to track landscape changes and coastal land loss from 1932 to 2010. More recently, object-based approaches are being refined to extract coastlines from high resolution satellite data (Giannini and Parente 2015).

*Unmanned Aircraft System applications in coastal research*

Unmanned Aircraft System (UAS) technology has expanded in recent years for various survey and mapping applications. In the late 1970s, Przybilla & Wester-Ebbinghaus (1979) first used a fixed wing remotely controlled aircraft in photogrammetry experiments. In 2004, Eisenbeiss, Lambers, & Sauerbier (2005) were the first to create a high-resolution digital terrain model using a commercial low-cost model helicopter with semiautomated navigation.

UAS technology has developed quickly since the turn of century and has witnessed unprecedented technological developments in computing, communications, navigation, control, and optics (Pereira et al. 2009). Chong (2007) used high definition video to map local beach erosion. Lejot et al. (2007) used very high spatial resolution imagery to map channel bathymetry and topography from a UAS platform. Light-weight multispectral sensors for UAS are being used increasingly (Laliberte et al. 2011). Niethammer, James, Rothmund, Travelletti, & Joswig (2012) used low-cost small digital camera to map landslide topography and create reasonably accurate digital terrain models. Multispectral and hyperspectral imagery are regularly being used to image, classify, and map wetlands (Phinn, Stow, and Zedler 1996; Chust et al. 2008; Yang and Artigas 2010; Lechner et al. 2012; Klemas 2013). UAS are now widely used in a host of environmental applications, such as coastal wetland mapping, LIDAR bathymetry, flood and wildfire surveillance, tracking oil spills, urban studies, and arctic ice investigations (Klemas 2015).

*Comparing UAS and other methods*

Comparing traditional ground surveys, aerial photogrammetry, and satellite data analysis is not straightforward. Each method has a niche and a best-fit for project application. There are various tradeoffs to consider such as cost, area covered, resolution, and the potential for high temporal sampling, etc. Manned aircraft overflights, for example, can be costly (Klemas 2013). UAS technology, however, can potentially drop the cost dramatically. GPS-guided UAS have the capacity to obtain very high spatial resolution (1-10 cm) imagery of specific landscape features with revisit times determined by the operator as opposed to fixed satellite revisit times (Lechner et al. 2012).

For coastal wetland monitoring in Louisiana, there are several examples of remote sensing data types, at various spatial scales, that can fill in the data gaps between the helicopter coastwide survey and the CRMS network stations. These include LANDSAT satellite imagery (30m), Worldview satellite imagery (3m), traditional aircraft captured aerial photography (1m), and UAS captured aerial photography (2cm). Figure 1 includes an examples of a typical aerial photography base map with 1 meter resolution compared to 2.5 cm resolution UAS imagery collected in the same location.


Figure 1: One-meter resolution aerial photography (below) collected as part of the Coastal Wetlands Planning, Protection and Restoration Act program (CWPPRA 2008) and UAS imagery collected in 2106 at the same location (above).

UAS technology has the additional advantage over traditional methods by allowing flexible deployments capable of acquiring both high-temporal and hyperspatial resolution data (Niethammer et al. 2012). Recent developments in UAS have sparked interest in the ability of these systems to fly the current Louisiana coastwide helicopter transects and to collect hyperspatial aerial images of the sampling sites. At present, the helicopter survey is conducted once every seven years by a crew of four, so a successful implementation of a UAS survey could increase the temporal resolution of the dataset and potentially reduce the cost of deployment. The ability to capture near-infrared reflectance of the sampling locations could also provide information on the health and vigor of the sampled vegetation using the Normalized Difference Vegetation Index (NDVI), which would be an improvement over current methods. Additional improvements that UAS imagery could provide include the ability to compute a Digital Surface Model (DSM) and to provide source data for image analysis techniques that could classify the collected imagery, automate the species identification process, and calculate various metrics that approximate ecosystem services.

## III. Research Objective

The goal of this project is to investigate the use of UAS and hyperspatial imagery collections for calculating species composition and ecosystem service metrics in a coastal Louisiana grass-dominated marsh. Specifically, the researchers were interested in improving monitoring techniques with UAS technology and developing methods to calculate biomass, productivity, species composition, and a land-water interface model. Such improvements would be important steps towards a comprehensive monitoring program of the Louisiana coastal zone and would provide useful tools to study how coastal wetland ecosystems respond to human perturbations.

A pilot project was conducted in Coastal Louisiana to collect hyperspatial/multispectral aerial imagery from a UAS to determine the feasibility of the technology for vegetation mapping and landscape analyses of ecosystem service metrics. Specifically, the team addressed the following research question: *Can UAS hyperspatial imagery be used to classify species composition, model the land-water interface, and quantify certain ecosystem services, specifically the Normalized Difference Vegetation Index (NDVI) and plant height, in a Spartina patens dominated brackish coastal marsh environment?*

To accomplish the project mission, the team had the following general workflow (Figure 2): 1) collect 2.5 cm resolution UAS imagery using red-green-blue and near-infrared sensors of a 1km2 area in a coastal Louisiana marsh, 2) create georeferenced orthomosaic and DSM raster datasets, 3) use Object-based image analysis to model the land-water interface, dominant species distribution, plant height, and NDVI.

## IV. Fieldwork

The project site was a degraded oligohaline wiregrass (fresh to intermediate) marsh located in Terrebonne Parish, Louisiana along the Northern Gulf of Mexico, north of Lake Boudreaux, and east of Bayou Grand Calliou (Figure 3). The site is part of the Terrebonne Bay drainage basin in the Mississippi River Deltaic Plain. The area is prone to high rates of subsidence due to compaction of Holocene alluvial sediments and movements of nearby faults. With the additive effects of eustatic sea level rise, nutria herbivory, and hydrologic modifications due to canal and embankment alterations in the landscape, this area has some of the highest rates of coastal land loss in the world. One benefit of this study area is that there is one long-term monitoring site belonging to the Coastwide Reference Monitoring System (Steyer 2010) within the project boundary. This station has on-the-ground sampling locations for species cover and was used as a reference dataset. The $1km^2$ area around CRMS Sites 0392 was the area of the data acquisition for this project (Figure 3).

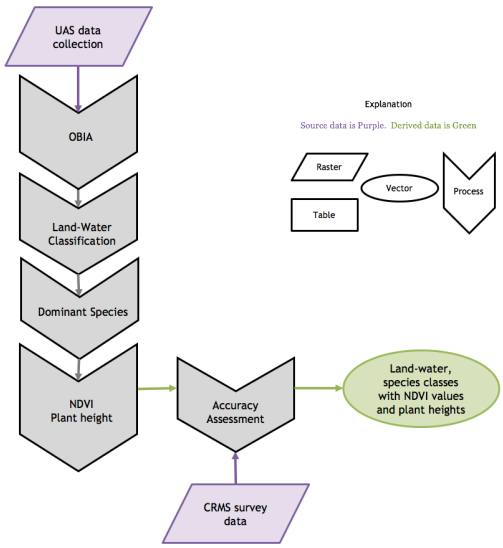


Figure 2: Project workflow diagram.

CRMS site 0392 was chosen with permission from the state governing agency and private landowner. Even though the site was in Class G airspace, the pilot in command coordinated with the Houma-Terrebonne Airport (HUM) because the site was under the Class E airspace surrounding HUM. All flight operations were compliant with the Federal Aviation Authority (FAA) Part 107 ruling, which incidentally was effective August 29, 2017. The fieldwork for this project was conducted August 29 and 30, 2017.

The area of interest (AOI) was divided into 3 flight blocks. Each block required approximately 35 minutes to complete, which allowed 15 minutes of additional flight time for emergency maneuvers and travel to the landing location. Because the AOI was over a coastal marsh, and because the marsh in question was highly degraded and broken, there was no logical landing location near the AOI. An appropriate landing location was identified 4 km north of the AOI. To maintain radio communications between the aerial rover and the ground control station, the project team chased the rover home to the landing location using an airboat.

Ground control point (GCP) photo targets were evenly placed throughout all three flight blocks (Figures 3 and 4). The shared boundaries of the flight blocks also shared ground control targets. The targets were vinyl sheets (2' x 2') with an iron cross pattern. The targets were fixed atop wooden stakes that were driven into the marsh and elevated so that the targets were visible over the marsh grass (Figure 5). A center stake was driven in the middle of the target to create a tent effect and fix the location of the center. The center point was then surveyed in using high accuracy GPS equipment (Figure 6, horizontal accuracy = 1cm and vertical accuracy = 2cm).

The team used a Trimble UX5 aerial imaging rover (Figure 7, http://uas.trimble.com/ux5). Payload sensors include the Sony α5100 with a red-green-blue (RGB) sensor and a Sony NEX-5r with a near infrared-red-green (NIR) sensor. The catapult launcher was secured to the bow of a research vessel and the UX5 was launched out over the water within the AOI. A belly landing was used to bring the rover back to the ground. This method has several drawbacks. A clear area roughly 50m long and 30m wide is necessary in the event of a wind gust or other malfunction during landing. The team could not find a suitable place with a large area of solid marsh grass within the AOI. Public lands north of the AOI, near the public boat launch was chosen for landing as mentioned above. Four flights were flown over the course of two days. The results presented here represent two of those flights, both of which are from the same flight block. One contains the RGB dataset and the other contains the NIR dataset.

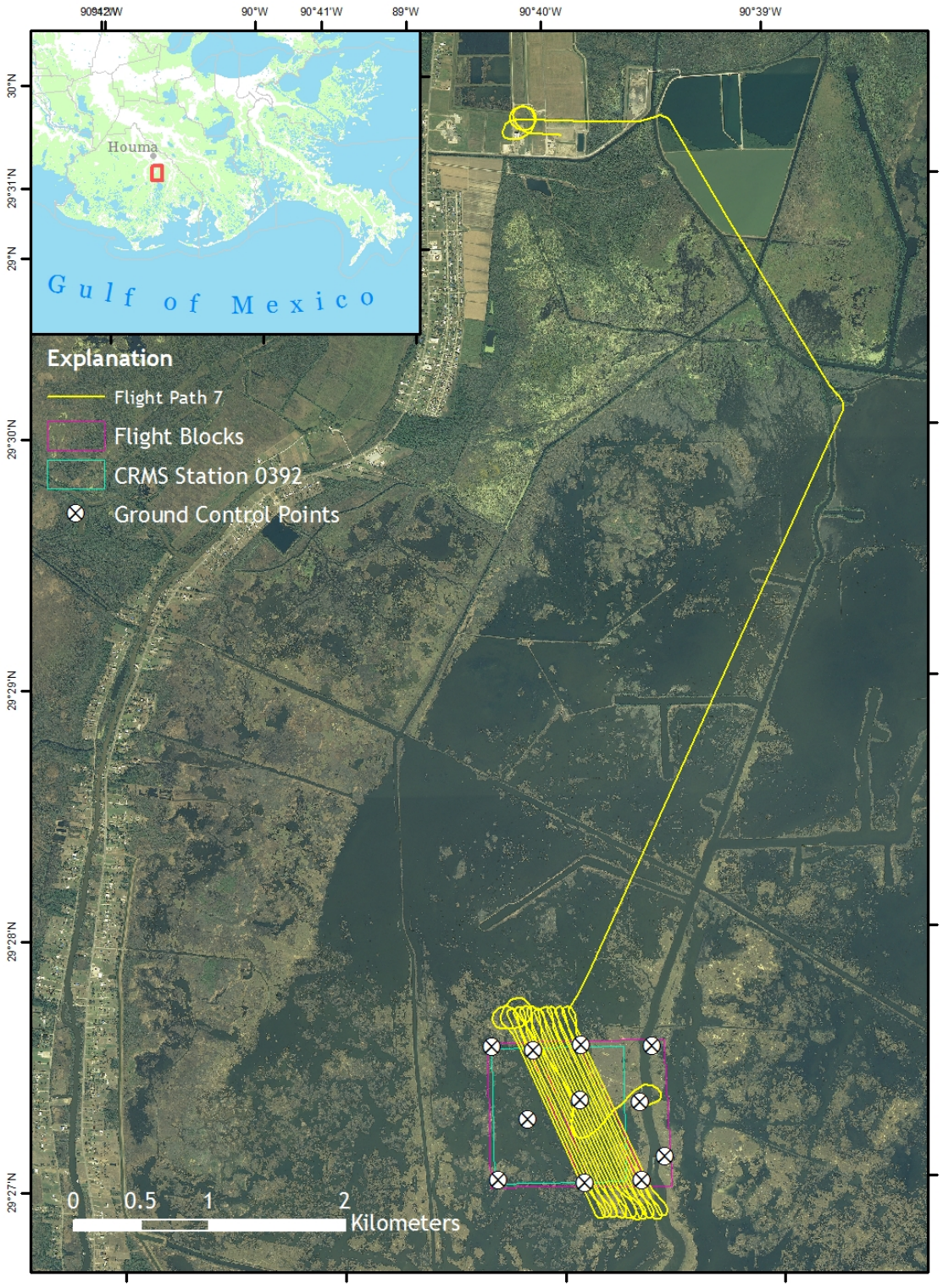


*Aerial Imagery: Coastal Wetlands Planning, Protection and Restoration Act (CWPPRA), 2008*

Figure 3: Location map of the project site including one set of flight lines in yellow, ground control points in white/black, and the 1km2 area of interest (AOI) surrounding CRMS 0392. The landing location is 4 km north of the AOI in an open upland field.

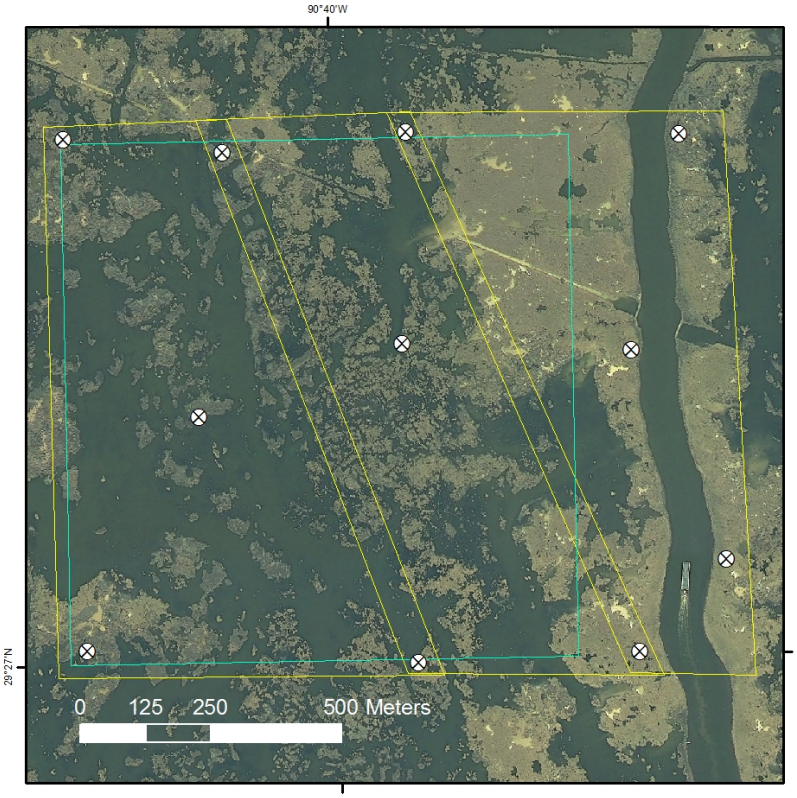


Figure 4: Location of ground control point photo targets in black and white as well as the flight blocks in yellow and the 1 $km^2$ buffer around CRMS 0392 in teal.

Figure 5: Example of a ground control point photo target.

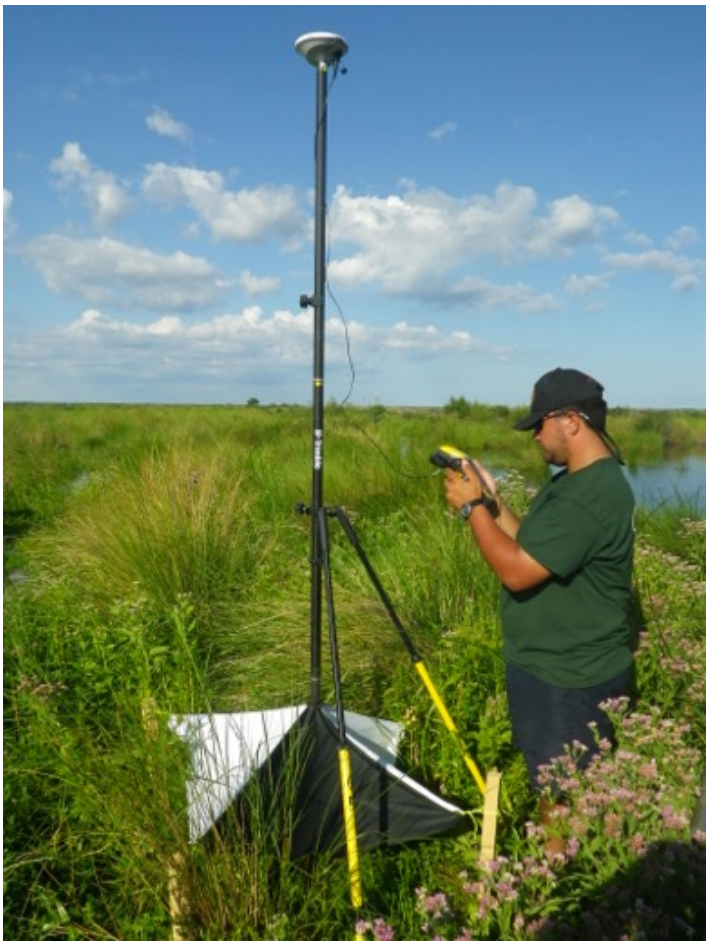

Figure 6: GPS Survey of a ground control point.

Figure 7: Trimble UX5 aerial imaging rover used in this project.

## V. Post-processing

Trimble UAS Master Inpho Software (Figure 8; Trimble Navigation Limited, 2016) was the photogrammetric software used to process the UAS imagery and generate orthomosaic and DSM raster datasets. Over 1000 images are collected per flight. Each image has an approximate latitude, longitude, altitude, roll, pitch, and yaw value associated with it. These initial approximations of the image's external orientation were used by the software to extract tie point locations, i.e. those locations that could be identified in multiple photos. The precise location of the ground control points (GCPs) were measured in all available images. Each GCP is measured (located) within each available picture to refine the initial orientation and to tightly georeference the orthomosaics to a datum (See Figure 9). After the absolute orientation process was completed, the root mean square error (RMSE) for the horizontal and vertical control was 2.40 cm and 2.42 cm, respectively. The 95% confidence level for the horizontal and vertical control was 4.83 cm and 4.74 cm, respectively. Final RGB, NIR, and DSM datasets are presented below in Figures 10, 11, and 12, respectively. The ground sample distance was as low as 2.6 cm for the orthomosaic and 7.2 cm for the digital surface model. These hyperspatial datasets allows a user to discern patterns and objects with detail. Even the shape and size of a broadleaf blade can be observed and calculated.

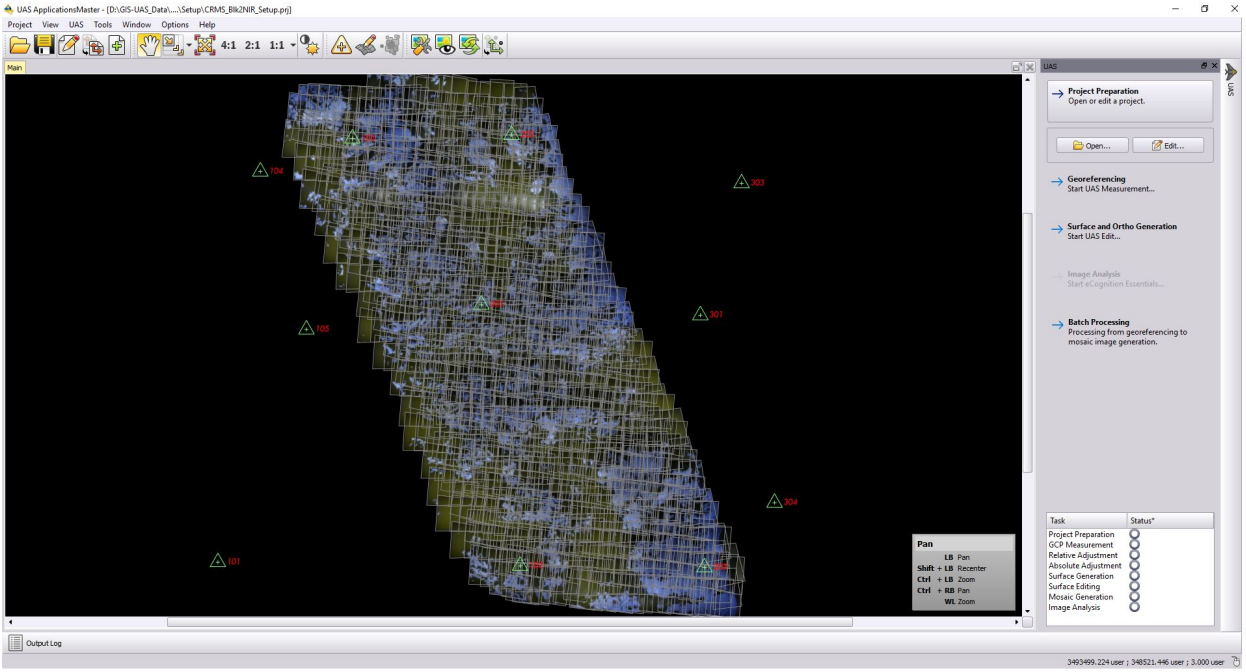


Figure 8: A screenshot of the Photogrammetry software Trimble UAS Master showing the wireframes of the raw NIR imagery, Ground Control Points, and orthomosaic overview.

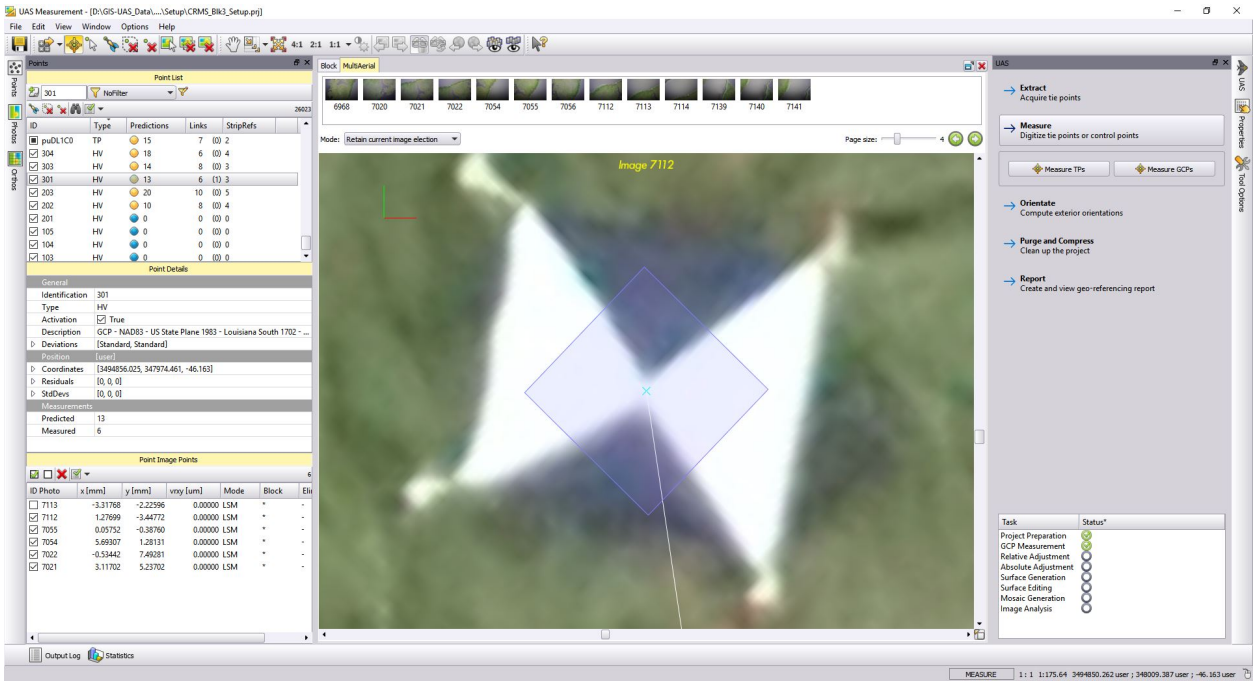


Figure 9: A screenshot of the Georeferencing Editor and the GCP/Manual Tie Point Table showing the location of a ground control point 301 in image 7112.

## VI. Object-based image analysis

UAS imagery has been analyzed using object-based image analysis (OBIA) classification methods in the past (e.g. Laliberte and Rango 2009; Laliberte and Rango 2011). Originally developed for 1 meter aerial photography, the ability of the method to downscale to UAS imagery is encouraging. With high resolution datasets, the spectral variance increases within target classes. Spectral separation between the classes is therefore more difficult to specify and classify (Marceau et al. 1999; Blaschke 2010). Similar to human interpretation, OBIA methods address these scaling issues by segmenting or grouping the finer pixels into image objects that are made up of multiple neighboring pixels sharing similar attributes such as spectral signature, texture, shape, and context to other objects (Blaschke 2010). This makes classification of UAS imagery easier because the programmer is then tasked with finding commonalities by object (100's to 1000's of pixels) rather than individual (2-3cm) pixels.

The goal of the OBIA in this study was the classification of marsh grass versus open water, the identification of dominant plant species, and the development of a Normalized Difference Vegetation Index (NDVI) surface model using hyperspatial, multispectral UAS imagery. The first step in the analysis was to classify objects as either land or water and then to classify land objects into one of three vegetation categories: 1) Grass, *Spartina patens),* 2) Reed, *Phragmites australis*, 3) Other, a mix of B*acopa spp., Plucheas spp., Iva spp., and Baccharis spp*. Figure 13 demonstrates the outlines of objects identified in the UAS imagery. The objects were delineated using Trimble eCognition Developer software ("eCognition Developer" 2016) based on similar spectral, texture, size, values as well as the context of other neighboring objects. Based on the characteristics of objects that shared a common target classification, a rule set was developed to methodically classify objects into one of the three target classes.


Figure 10: RGB dataset generated from UAS imagery over the project site.

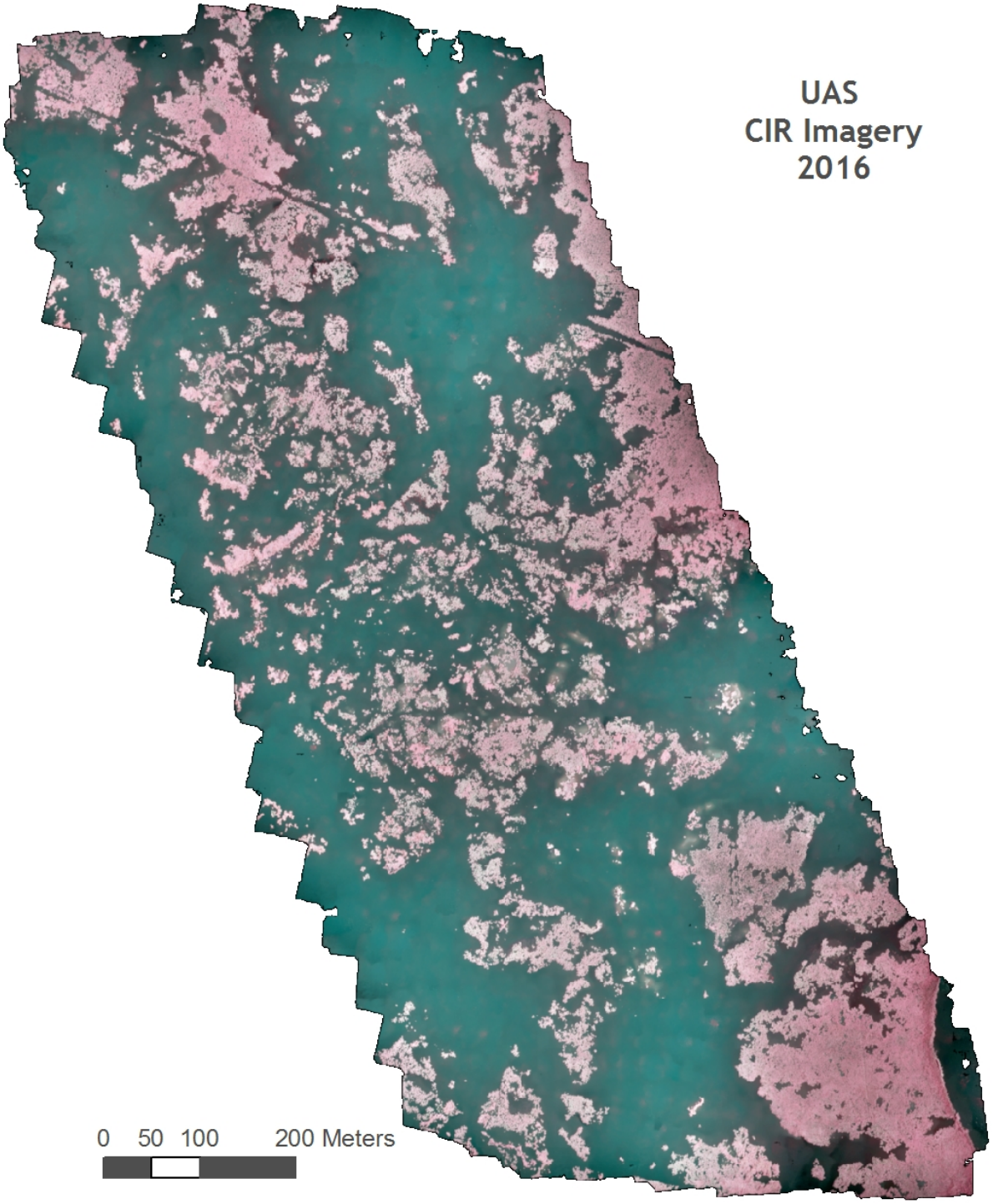


Figure 11: NIR dataset generated from UAS imagery over the project site.

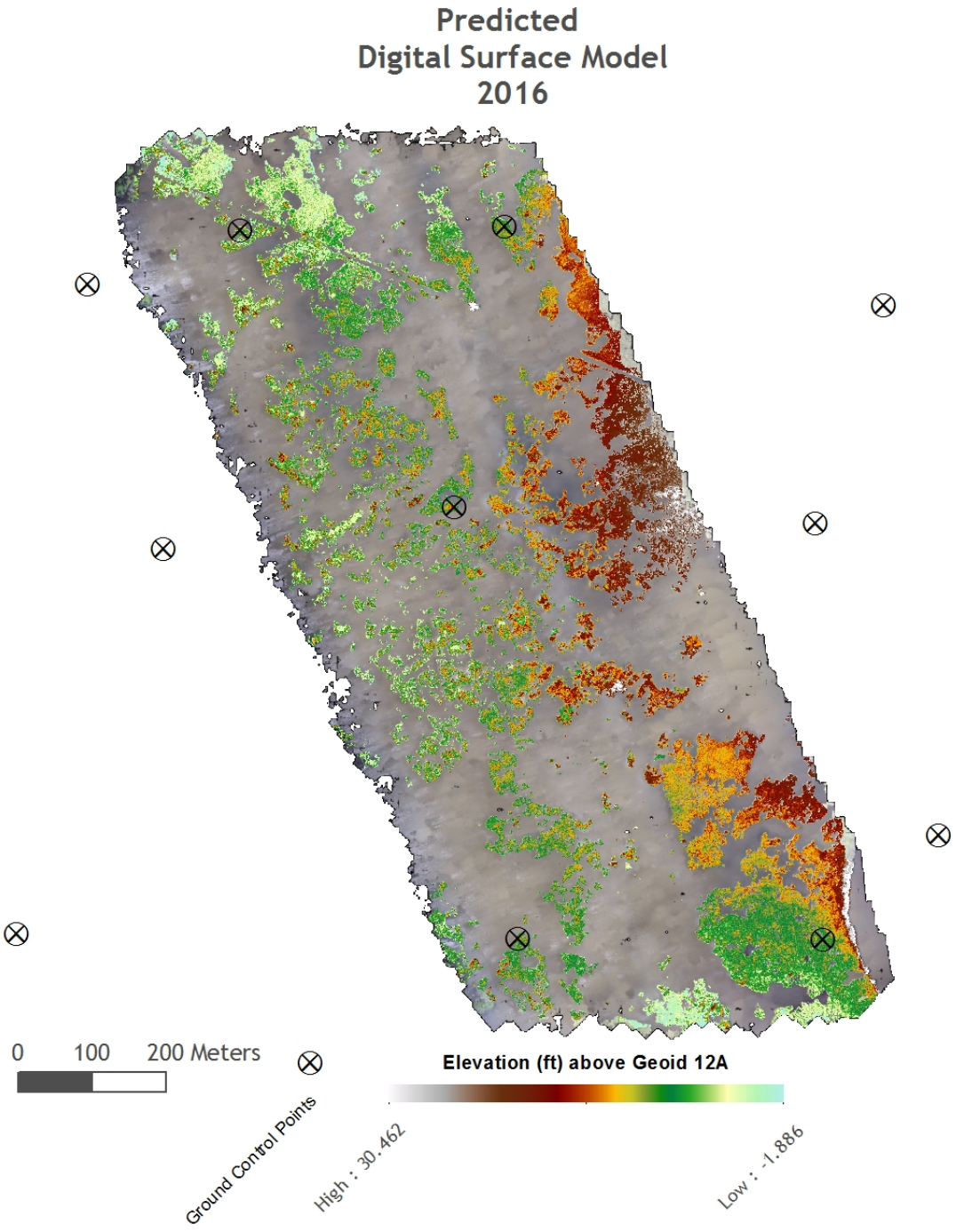


Figure 12: DSM dataset generated from UAS imagery over the project site.

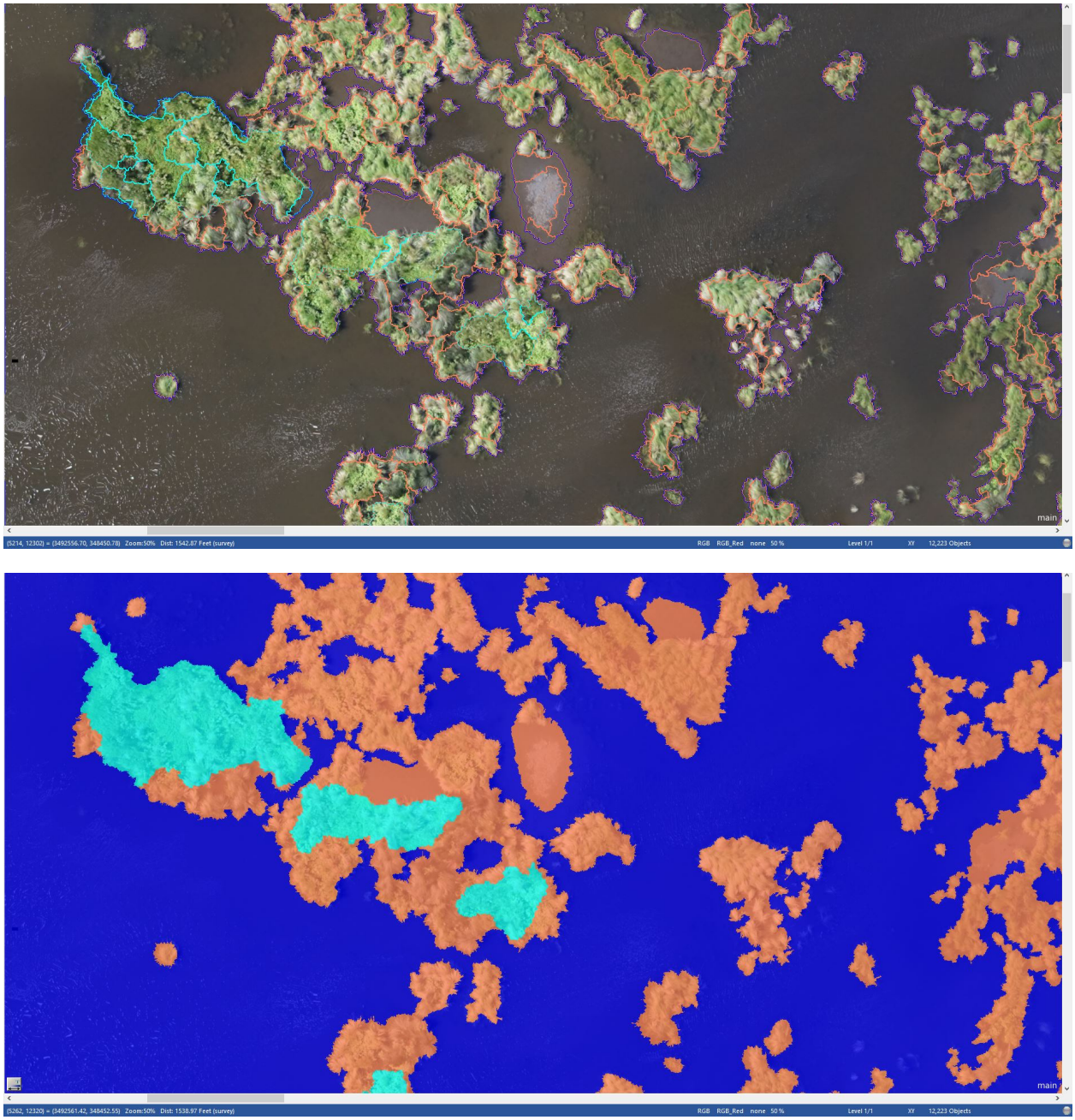

Figure 13: Objects outlined (above) and then classified (below). Blue is the class Water, teal is the class Other, and orange is the class Grass.

The reflectance values of the near infrared spectrum coupled with the hyperspatial resolution of the UAS imagery made the identification of the water objects fairly easy. Using a simple threshold level, those objects with a mean near-infrared reflectance value less than 90 were classified as water (because water absorbs near infrared wavelengths). For the dominant vegetation species identification, the algorithms focused primarily on height, texture, and greenness. Because the common reed *Phragmites australis* is a tall, clumping species, this Reed class was primarily identified by height (i.e. objects that were taller than their surrounding objects). The Other class was primarily identified by greenness because this class of

plants were generally greener than the surrounding grasses. After classifying both the Reed and Other classes, the remaining objects belonging to the larger Land class were then classified as Grass.

*NDVI*

The reflectance index NDVI is regularly used in coastal and upland vegetation analyses to indicate the greenness and general health of the vegetation (Steyer, Couvillion, and Barras 2013; Carle and Sasser 2016; Tucker 1979). NDVI values were calculated for each pixel of the NIR orthomosaic as the ratio of the near-infrared and red reflectance (Tucker 1979). Results from this analysis are presented in Figure 14. Note the highest NDVI values in the southeast corner of the project area. This is a high marsh adjacent to a distributary channel, presumably with good tidal exchange and oxygenated soils.

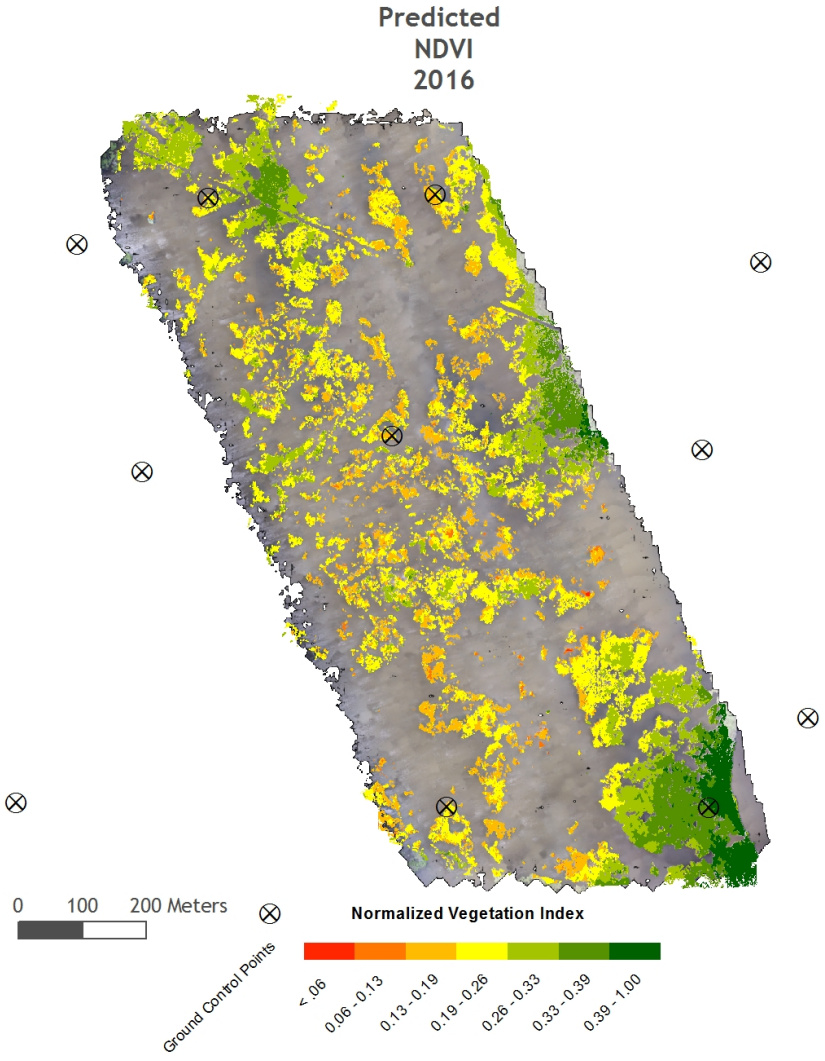


Figure 14: NDVI surface model of the project area.

## VII. Accuracy Assessment

*Standard vegetation assessment*

An accuracy assessment was then performed using two methods. The first is a stratified random sampling in which a predetermined number of random x,y points were selected within each group (50 Water, 50

Grass, 20 Other, and 10 Reed). The researchers then used the original UAS orthomosaics to determine if the model was properly classified at each point. Results are presented as an error matrix in Table 1. Overall accuracy was 85% and the Kappa Coefficient was 0.78. These values are within an acceptable range for traditional image analysis. User's Accuracy ranged from 67% for Other to 100% for Reed. Producer's Accuracy ranged from 73% for Grass to 100% for Water. This Producer's Accuracy for Water is noteworthy because it means that the simple approach to classifying water, i.e. a single threshold of near-infrared reflectance, is satisfactory. The fine-scaled, 2-6cm, delineation between the land-water interface is a significant improvement in coastal land loss mapping efforts. Each 2-6 cm pixel is either land or water. There is very little mixing of spectral signatures within UAS orthophoto pixels as compared to the mixing found in traditional 1 m aerial photographs (Figure 1). As such, the land-water interface model is highly accuracy and reliable.

| | | Reference Class | | | | | |
|---|---|---|---|---|---|---|---|
| | | 1) Water | 2) Grass | 3) Other | 4) Reed | Count | Producer's Accuracy |
| Predicted Class | 1) Water | **49** | 0 | 0 | 0 | 49 | 100% |
| | 2) Grass | 7 | **35** | 6 | 0 | 48 | 73% |
| | 3) Other | 2 | 2 | **16** | 0 | 20 | 80% |
| | 4) Reed | 0 | 0 | 2 | **8** | 10 | 80% |
| | Count | 58 | 37 | 24 | 8 | 127 | |
| | User's Accuracy | 84% | 95% | 67% | 100% | | |

Overall Accuracy: 85%
Kappa Coefficient: 0.78

Table 1: Error matrix demonstrating the results from the accuracy assessment of the object-based image analysis.

*Comparison with CRMS data*

Previously acquired field data from the CRMS site 0932 were then compared with the models generated for this project. Specifically, the researchers compared predicted percent land versus measured percent land, predicted vegetation class versus observed vegetation class, and predicted plant height versus measured plant height. CRMS data were collected at three subsample sites along a transect within the CRMS 0932 boundary (Figure 15). The subsample sites are 4 $m^2$ quadrants whose locations were measured using a handheld GPS in the field with roughly 3 m accuracy.

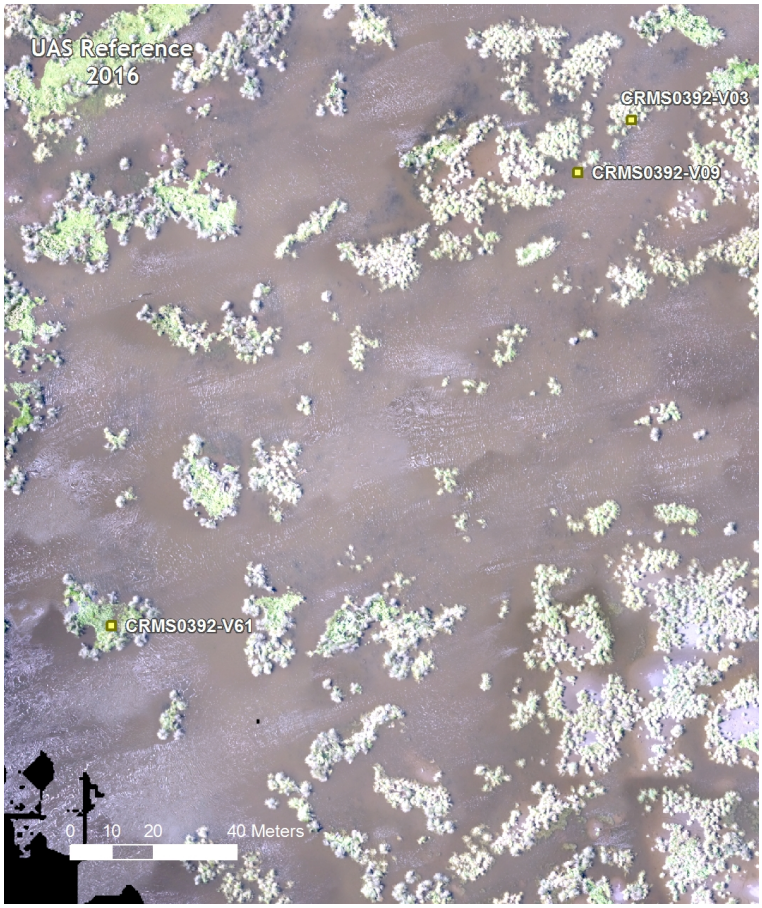


Figure 15: Three subsample sites (V03, V09, and V61) in the project area.

*Land-water analysis*

The percent of each 4 $m^2$ quadrant occupied by land was compared between the predicted land-water model generated from UAS imagery (Figure 16) and a similar dataset that is generated by the CRMS team and delivered through the CRMS database (Figure 17, CPRA 2012). The CRMS land-water analysis is a pixel-based analysis using aerial photographs with roughly 1 meter ground sample distance. The analysis presented here is an object-based image analysis using aerial photography with roughly 2.5cm ground sample distance. Results of this comparison are presented in Table 2.

Given the substantial difference in resolution between the two datasets, and the difficulties in delineating the land-water interface when 1 m pixels along the marsh edge are a mix of land and water signatures, the estimates of percent land were generally good for two of the three sites. The unsatisfactory site had a small percentage of land estimated by the CRMS model and a large percentage of land estimated by the UAS model. This could be explained by a georeferencing error, by the fact that only 4 pixels in the CRMS model constitute the 4 $m^2$ quadrant that was used to query the datasets, or by the difficulties mentioned above regarding delineating the land-water boundary.

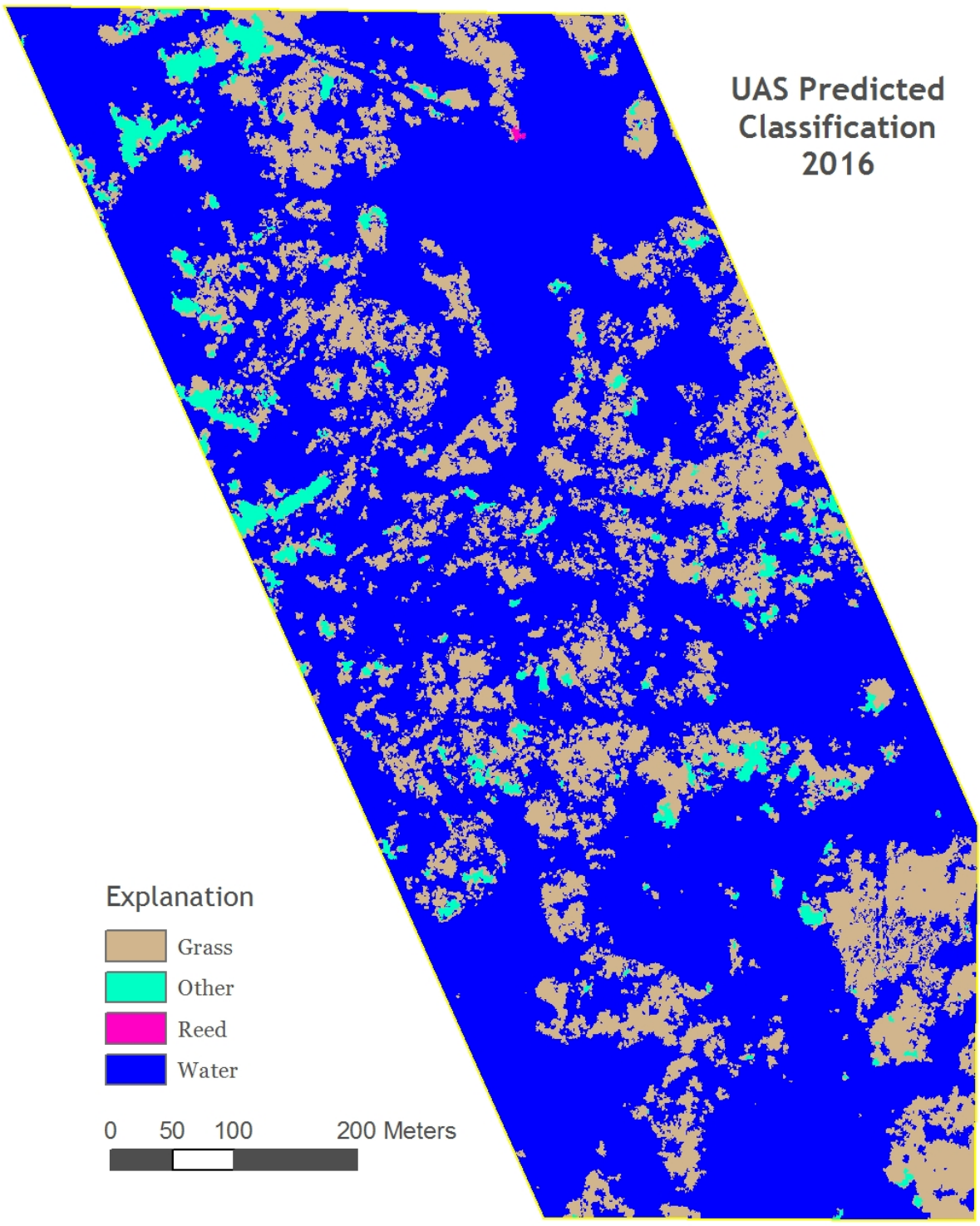


Figure 16: Vegetation model classified from showing the predicted land-water interface and dominant vegetation communities.

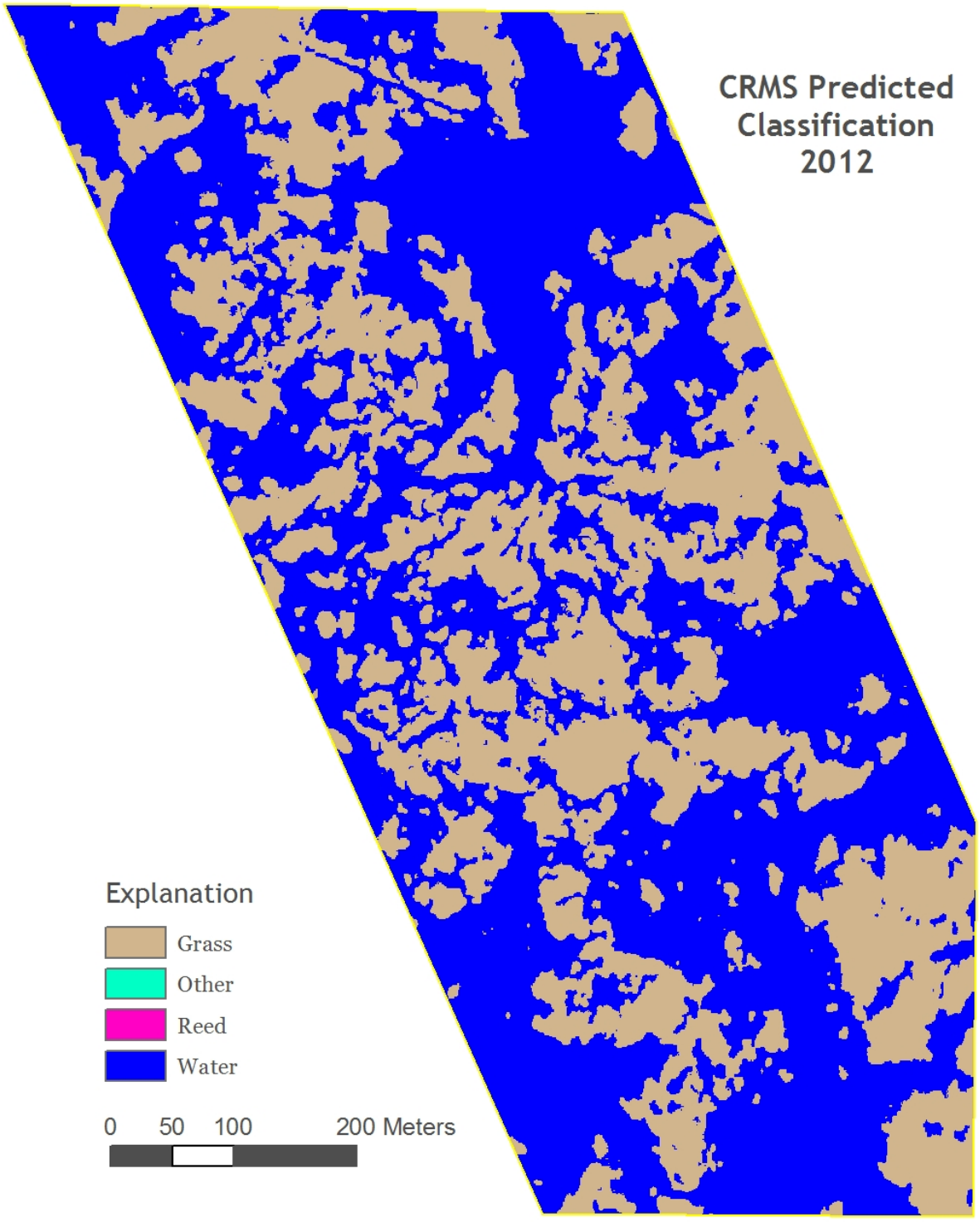


Figure 17: Land-water analysis model classified from 1m resolution aerial photography that is publically available through the CRMS program and.

| | % Land | | |
|---|---|---|---|
| | CRMS | Predicted | Fit |
| V03 | 5% | 94% | +89% |
| V09 | 1% | 8% | +7% |
| V61 | 100% | 94% | -6% |

Table 2: Results of the land-water classification comparison between the predicted land-water interface model and the publically-available CRMS land-water analysis dataset.

*CRMS vegetation classification*

Vegetation communities were compared between the predicted vegetation model and the observed CRMS data at each of three subsample sites located within the CRMS 0392 boundary (Figure 15). The predicted vegetation model was queried at each location and compared to the percent cover values reported in the CRMS dataset. Results of this comparison are presented in Table 3. For each sampled location, the modeled dominant vegetation matched the observed dominant vegetation on the ground.

| | Vegetation Classification | | | Notes |
|---|---|---|---|---|
| | CRMS | Predicted | Fit | |
| V03 | Grass | Grass | 100% | Amaranthus, Patens, Cyperus mix |
| V09 | Grass | Grass | 100% | Patens clump |
| V61 | Other | Other | 100% | Bacopa, Eleocharis, Pluchea mix |

Table 3: Results of the vegetation classification comparison between the predicted vegetation model and the observed cover values reported in the CRMS dataset.

*Plant height*

Plant height was estimated as the difference between the modeled DSM (i.e. the elevation of the tops of the plants) and the elevation of the marsh surface. To estimate the marsh surface, an inverse distance weighted method was used to model marsh elevation based on GPS measurements collected when the ground control points were surveyed (Figure 18). Predicted plant height was then calculated as the difference between the cell value of the DSM generated from the UAS imagery and the predicted marsh elevation raster model (Figure 19). The model was then queried at the 3 subsample locations where the CRMS ground crew surveyed marsh vegetation and measured mean plant height (Figure 15). Results of this comparison are presented in the third and fourth columns of Table 4.

The CRMS field crews also estimated average marsh elevation based on their GPS surveys. Their estimates are based on multiple points (mean elevation = 0.229 ft above Geoid12A) and are thought to be more robust than the single point measurements that this project team collected. For this reason, a second estimate of plant height was calculated as the difference between the cell value of the DSM at each sample location and the estimated CRMS-based marsh elevation value for the site. Results of this comparison are presented in the fifth and sixth columns of Table 4.

Estimates of plant height were generally good for two of the three sites. The unsatisfactory site had a small percentage of land predicted. Because the locations of the subsample sites were determined using rough GPS estimations (3m), it is highly unlikely that the modeled dataset was queried in the exact location as the sites on the ground. A 3 m distance can easily traverse open water, partial plant cover, and complete plant cover in this highly-degraded landscape. In aggregate, however, the methodology shows promise in its ability to estimate plant height at the landscape scale.

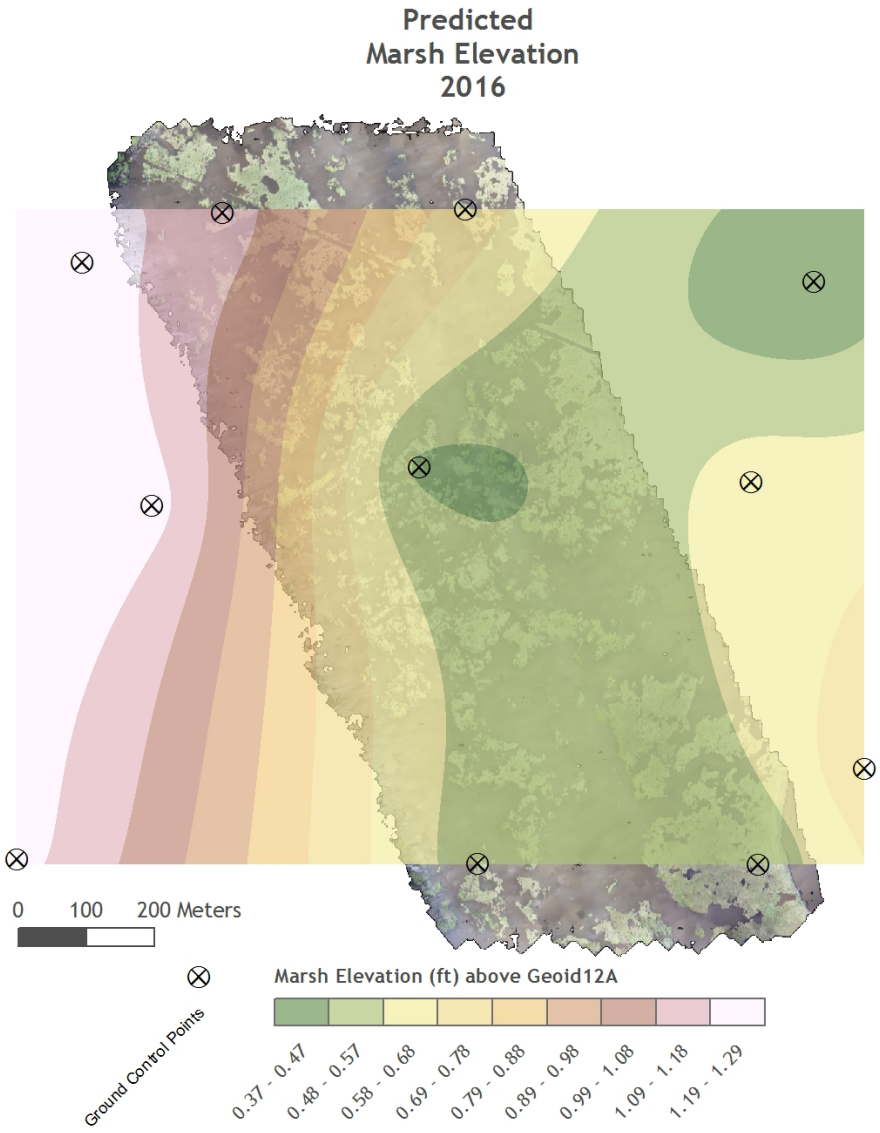


Figure 18: Predicted marsh elevation surface.

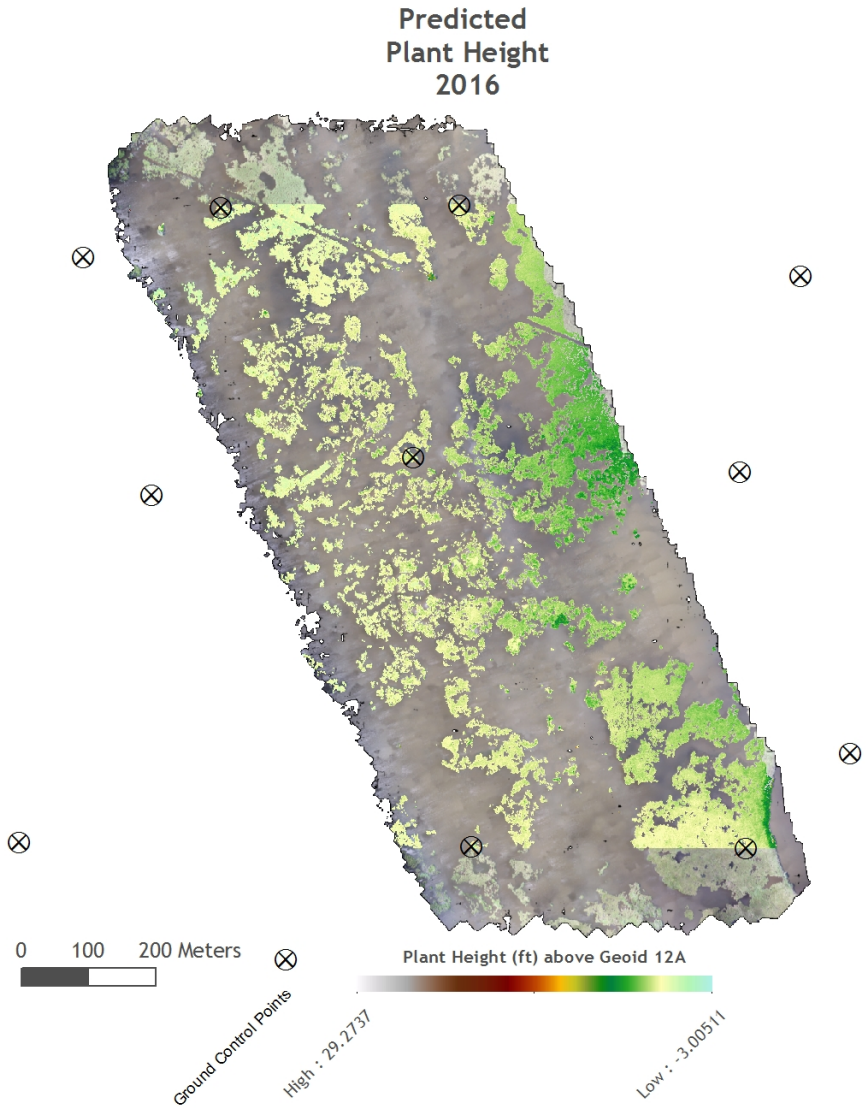


Figure 19: Predicted plant height.

| | Maximum Plant Height (ft) | | | | |
|---|---|---|---|---|---|
| | CRMS | Predicted (diff. **modeled** marsh elev.) | Fit | Predicted (diff. **measured** marsh elev.) | Fit |
| V03 | 4.84 | 3.97 | 82% | 4.26 | 88% |
| V09 | 3.91 | 0.86 | 22% | 1.406 | 36% |
| V61 | 1.6 | 1.19 | 74% | 1.504 | 94% |

Table 4: Results of the predicted and measured plant height estimates for three subsample site locations at CRMS 0392.

## VIII. Discussion

One reason for a lower user's accuracy, particularly for the water class, is the ability of the researcher to observe objects with great detail during the accuracy assessment. For example, the OBIA rule set classified the point shown in Figure 20 as land, but inspection of the hyperspatial imagery shows the grass stems and leaves are actually extending over water. So, this point predicted Grass but the reference class was Water at the ground level and was reported as a missed classification. The scale of this kind of analysis and accuracy assessment, however, is novel to hyperspatial datasets and something that will set the subdiscipline apart from traditional analysis of 1m aerial photographs.

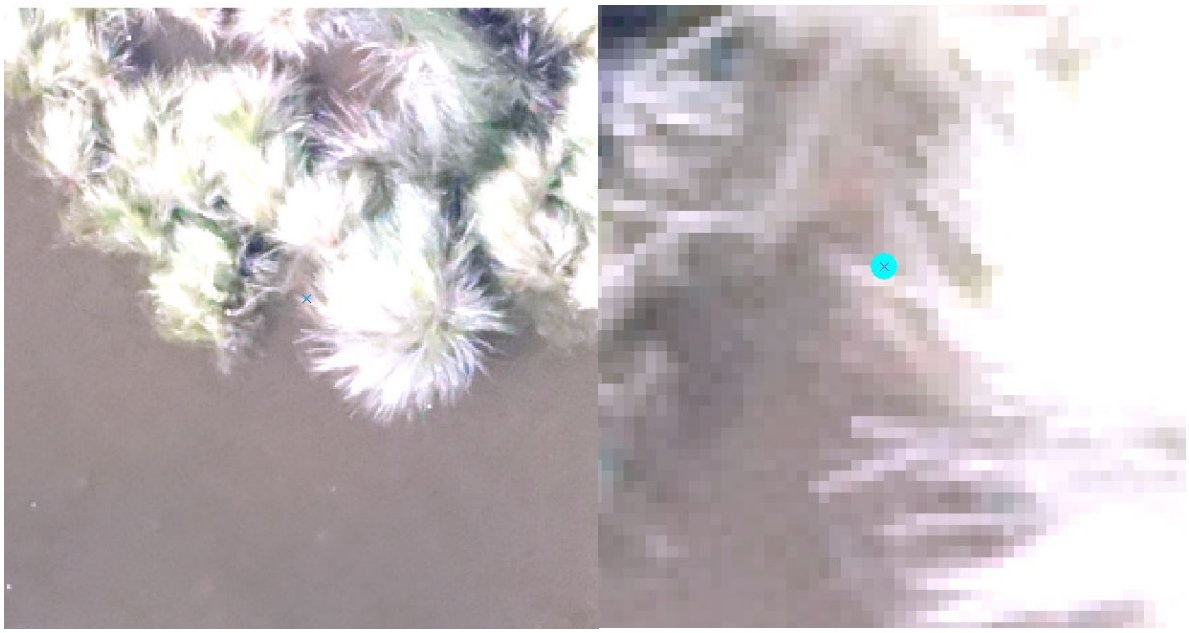

Figure 20: An example of a user's error where the selected point is classified as Grass, but the reference class is Water. The researcher can discern the true reference class only because of the hyperspatial nature of the dataset.

Further research is need to refine the algorithms and rule sets for accurate predictions and classifications of UAS image datasets. Additionally, radiometric corrections and standards will need to be set for larger regional analyses. The brightness and radiometry of UAS imagery are highly variable because of changing sun angles and weather patterns throughout a single flight mission or multiple missions from day to day. This variability in the raw imagery will need to be addressed if standardized approaches at larger regional scales are desired.

Another area in need of further research is the estimation of plant biomass and carbon sequestration rates based on the UAS imagery and subsequent datasets. Presumably, if one can correctly classify the dominant plant species and plant height of an object, then some standard coefficients could be used to calculate the biomass, productivity, and carbon sequestration. These coefficients would be based on experimental and observational datasets, and would be dependent on the local conditions of the site in question. The ability to scale up field-based measurements to regional models, however, remains a worthy goal.

*Lessons Learned*

Operating a UAS in a coastal environment does not come without worry or problems. Issues to consider include proper locations for takeoff and landing, properly estimating flight times that account for high wind conditions, and communicating with local land owners regarding privacy and permission concerns. Current FAA regulations constrain the UAS to only fly within the line of sight of the pilot in command or designated spotter. If future regulations relax this requirement to allow beyond line of sight operations, the ability to work from an upland site and capture imagery over coastal wetland sites will be easier and perhaps worthy of long-range, high-endurance UAS investments.

These limitations notwithstanding, there are several benefits to be gained from the use of UAS in coastal research. These operations could save time and money when compared to field surveys of elevation and vegetation. When in the field, there are fewer personnel requirements (1-2 persons minimum). UAS can overcome site accessibility issues such as low water offsetting the need for airboat access. From a data deliverable perspective, UAS can deliver more frequent monitoring events and develop higher resolution structural models, surface elevation models, and multispectral orthomosaics of entire project sites. In the case of the CRMS monitoring framework, these datasets can capture previously unknown variability in the landscape by generating 1 $km^2$ continuous surface models as opposed to the current dataset of ten 4 $m^2$ plots per site.

Finally, the ability to generate high resolution maps of the land-water interface, land loss, and habitat fragmentation are particularly exciting. The scale of such assessments could not, at present, be coast-wide or even regional. But the potential is there to slowly start increasing the foot print of these kinds of analyses, especially as technology advances in both long-distance UAS operations and big data analysis.

## IX. References


Baker, MC, MA Steinhoff, and GF Fricano. 2016. "Integrated Effects of the Deepwater Horizon Oil Spill on Nearshore Ecosystems." *Marine Ecology Progress Series* View: 1–16. doi:10.3354/meps11920.

Barbier, Edward B., Sally D. Hacker, Chris Kennedy, Evamaria W. Koch, Adrian C. Stier, and Brian R. Silliman. 2011. "The Value of Estuarine and Coastal Ecosystem Services." *Ecological Monographs* 81 (2): 169–93. doi:10.1890/10-1510.1.

Bell, Frederick W. 1997. "The Economic Valuation of Saltwater Marsh Supporting Marine Recreational Fishing in the Southeastern United States." *Ecological Economics* 21 (3). Elsevier: 243–54. doi:10.1016/s0921-8009(96)00105-x.

Belluco, Enrica, Monica Camuffo, Sergio Ferrari, Lorenza Modenese, Sonia Silvestri, Alessandro Marani, and Marco Marani. 2006. "Mapping Salt-Marsh Vegetation by Multispectral and Hyperspectral Remote Sensing." *Remote Sensing of Environment* 105 (1): 54–67. doi:10.1016/j.rse.2006.06.006.

Blaschke, T. 2010. "Object Based Image Analysis for Remote Sensing." *ISPRS Journal of Photogrammetry and Remote Sensing* 65 (1). Elsevier B.V.: 2–16. doi:10.1016/j.isprsjprs.2009.06.004.

Brooks, Robert P, G P Patil, Songlin Fei, Alix I Gitelman, Wayne L Myers, and Euan D Reavie. 2007. "Next Generation of Ecological Indicators of Wetland Condition." *EcoHealth* 4 (2): 176–78. doi:10.1007/s10393-007-0104-6.

Carle, Melissa Vernon, and Charles E. Sasser. 2016. "Productivity and Resilience: Long-Term Trends and Storm-Driven Fluctuations in the Plant Community of the Accreting Wax Lake Delta." *Estuaries and Coasts* 39 (2): 406–22. doi:10.1007/s12237-015-0005-9.

Chong, A.K. 2007. "HD Aerial Video for Coastal Zone Ecological Mapping." In *The 19th Annual Colloquium of the Spatial Information Research Centre*.

Chust, Guillem, Ibon Galparsoro, Ángel Borja, Javier Franco, and Adolfo Uriarte. 2008. "Coastal and Estuarine Habitat Mapping, Using LIDAR Height and Intensity and Multi-Spectral Imagery." *Estuarine, Coastal and Shelf Science* 78 (4): 633–43. doi:10.1016/j.ecss.2008.02.003.

Coastal Protection and Restoration Authority of Louisiana. 2012. *Louisiana's Comprehensive Master Plan for a Sustainable Coast*. Baton Rouge, LA: Coastal Protection and Restoration Authority of Louisiana. coastal.louisiana.gov.

Costanza, Robert, Ralph Arge, Rudolf De Groot, Stephen Farberk, Monica Grasso, Bruce Hannon, Karin Limburg, et al. 1997. "The Value of the World ' S Ecosystem Services and Natural Capital." *Nature* 387 (May): 253–60. doi:10.1038/387253a0.

Costanza, Robert, Octavio Pérez-Maqueo, M. Luisa Martinez, Paul Sutton, Sharolyn J. Anderson, and Kenneth Mulder. 2008. "The Value of Coastal Wetlands for Hurricane Protection." *AMBIO: A Journal of the Human Environment* 37 (4): 241–48. doi:10.1579/0044-7447(2008)37[241:TVOCWF]2.0.CO;2.

Couvillion, Brady R., Holly Beck, Donald Schoolmaster, and Michelle Fischer. 2016. "Land Area Change in Coastal Louisiana ( 1932 to 2016 ) Scientific Investigations Map 3381." *U.S. Geological Survey Scientific Investigations Map 3381*. https://doi.org/10.3133/ sim3381.

Couvillion, Brady Randall, John A Barras, Gregory D Steyer, William Sleavin, Michelle Fischer, Holly Beck, Nadine Trahan, Brad Griffin, and David Heckman. 2011. "Land Area Change in Coastal Louisiana (1932 to 2010)," 529.

CPRA - Coastal Protection and Restoration Authority of Louisiana. 2012. "CRMS0392 2012 Land-Water Analysis." Coastal Protection and Restoration Authority. https://www.lacoast.gov/crms2/crmsProducts.aspx?PRODTYPE=eLW. .

Craft, Christopher. 2007. "Freshwater Input Structures Soil Properties, Vertical Accretion, and Nutrient Accumulation of Georgia and U.S. Tidal Marshes." *Limnology and Oceanography* 52 (3): 1220–30. doi:10.4319/lo.2007.52.3.1220.

Craft, Christopher, Jonathan Clough, Jeff Ehman, Samantha Jove, Richard Park, Steve Pennings, Hongyu Guo, and Megan Machmuller. 2009. "Forecasting the Effects of Accelerated Sea-Level Rise on Tidal Marsh Ecosystem Services." *Frontiers in Ecology and the Environment* 7 (2): 73–78. doi:10.1890/070219.

CWPPRA - Coastal Wetlands Planning Protection and Restoration Act. 2008. "Louisiana Aerial Photography: 2008 DOQQs."

Day, John W., Louis D. Britsch, Suzanne R. Hawes, Gary P. Shaffer, Denise J. Reed, Donald Cahoon, Louis D. Britsch, Denise J. Reed, Suzanne R. Hawes, and Donald Cahoon. 2000. "Pattern and Process of Land Loss in the Mississippi Delta: A Spatial and Temporal Analysis of Wetland Habitat Change." *Estuaries* 23 (4): 425. doi:10.2307/1353136.

"eCognition Developer." 2016. Trimble Navigation Limited. http://www.ecognition.com/suite/ecognition-developer.

Eisenbeiss, Henri, Karsten Lambers, and Martin Sauerbier. 2005. "Photogrammetric Recording of the Archaeological Site of Pinchango Alto (Palpa, Peru) Using a Mini Helicopter (UAV)." *Annual Conference on Computer Applications and Quantitative Methods in Archaeology CAA*, no. March 2005: 21–24. http://www.photogrammetry.ethz.ch/general/persons/karsten/paper/eisenbeiss_et_al_2007.pdf.

Freeman III, A. Myrick. 1991. "Valuing Environmental Resources under Alternative Management Regimes." *Ecological Economics* 3 (3): 247–56.

Giannini, Massimiliano Basile, and Claudio Parente. 2015. "An Object Based Approach for Coastline Extraction from Quickbird Multispectral Images." *International Journal of Engineering and Technology* 6 (6): 2698–2704.

Gilmore, Martha S., Emily H. Wilson, Nels Barrett, Daniel L. Civco, Sandy Prisloe, James D. Hurd, and Cary Chadwick. 2008. "Integrating Multi-Temporal Spectral and Structural Information to Map Wetland Vegetation in a Lower Connecticut River Tidal Marsh." *Remote Sensing of Environment* 112 (11): 4048–60. doi:10.1016/j.rse.2008.05.020.

Hestir, Erin L., Shruti Khanna, Margaret E. Andrew, Maria J. Santos, Joshua H. Viers, Jonathan A. Greenberg, Sepalika S. Rajapakse, and Susan L. Ustin. 2008. "Identification of Invasive Vegetation Using Hyperspectral Remote Sensing in the California Delta Ecosystem." *Remote Sensing of Environment* 112 (11): 4034–47. doi:10.1016/j.rse.2008.01.022.

Klemas, Victor. 2013. "Airborne Remote Sensing of Coastal Features and Processes: An Overview."

*Journal of Coastal Research* 29 (2): 239–55. doi:10.2112/JCOASTRES-D-12-00107.1.

Klemas, Victor V. 2015. "Coastal and Environmental Remote Sensing from Unmanned Aerial Vehicles: An Overview." *Journal of Coastal Research* 315 (5): 1260–67. doi:10.2112/JCOASTRES-D-15-00005.1.

Laliberte, Andrea S., Mark A. Goforth, Caitriana M. Steele, and Albert Rango. 2011. "Multispectral Remote Sensing from Unmanned Aircraft: Image Processing Workflows and Applications for Rangeland Environments." *Remote Sensing* 3 (11): 2529–51. doi:10.3390/rs3112529.

Laliberte, Andrea S., and Albert Rango. 2009. "Texture and Scale in Object-Based Analysis of Subdecimeter Resolution Unmanned Aerial Vehicle (UAV) Imagery." *IEEE Transactions on Geoscience and Remote Sensing* 47 (3): 1–10. doi:10.1109/TGRS.2008.2009355.

———. 2011. "Image Processing and Classification Procedures for Analysis of Sub-Decimeter Imagery Acquired with an Unmanned Aircraft over Arid Rangelands." *GIScience & Remote Sensing* 48 (1): 4–23. doi:10.2747/1548-1603.48.1.4.

Lechner, a. M., A. Fletcher, K. Johansen, and P. Erskine. 2012. "Characterising Upland Swamps Using Object-Based Classification Methods and Hyper-Spatial Resolution Imagery Derived From an Unmanned Aerial Vehicle." *ISPRS Annals of Photogrammetry, Remote Sensing and Spatial Information Sciences* I-4 (September): 101–6. doi:10.5194/isprsannals-I-4-101-2012.

Lejot, J, C Delacourt, H Piégay, T Fournier, M-L. Trémélo, and P Allemand. 2007. "Very High Spatial Resolution Imagery for Channel Bathymetry and Topography from an Unmanned Mapping Controlled Platform." *Earth Surface Processes and Landforms* 32 (11). Wiley Online Library: 1705–25. doi:10.1002/esp.1595.

Marceau, D., D. Marceau, G.J. Hay, and G.J. Hay. 1999. "Contributions of Remote Sensing to the Scale Issue." *Canadian Journal of Remote Sensing* 25 (4): 357–66. http://www.geog.umontreal.ca/gc/people/danielle/..%5C..%5CPDFs%5CRspaper.htm.

Mitsch, William J., and James G. Gosselink. 2007. "Wetlands, Fourth Edition." Hoboken, New Jersey: John Wiley & Sons, Inc.

Moreau, Sophie, and Thuy Le Toan. 2003. "Biomass Quantification of Andean Wetland Forages Using ERS Satellite SAR Data for Optimizing Livestock Management." *Remote Sensing of Environment* 84 (4): 477–92. doi:10.1016/S0034-4257(02)00111-6.

Niethammer, U., M. R. James, S. Rothmund, J. Travelletti, and M. Joswig. 2012. "UAV-Based Remote Sensing of the Super-Sauze Landslide: Evaluation and Results." *Engineering Geology* 128. Elsevier B.V.: 2–11. doi:10.1016/j.enggeo.2011.03.012.

Pereira, E, R Beneatel, J Correia, L Felix, G Goncalves, J Morgado, and J Sousa. 2009. "Unmanned Air Vehicles for Coastal and Environmental Research." *Journal of Coastal Research* 2009 (56): 1557–61.

Phinn, S. R., D.A. Stow, and J.B. Zedler. 1996. "Monitoring Wetland Habitat Restoration in Southern California Using Airborne Multi Spectral Video Data." *Restoration Ecology* 4 (4): 412–22. doi:10.1111/j.1526-100X.1996.tb00194.x.

Przybilla, H.-J., and W. Wester-Ebbinghaus. 1979. "Bildflug Mit Ferngelenktem Kleinflug- Zeug."

*Bildmessung Und Luftbildwesen Zeitschrift Fuer Photogrammetrie Ferner- Kundung* 47 (5): 137–142.

Rebelo, L. M., C. M. Finlayson, and N. Nagabhatla. 2009. "Remote Sensing and GIS for Wetland Inventory, Mapping and Change Analysis." *Journal of Environmental Management* 90 (7). Elsevier Ltd: 2144–53. doi:10.1016/j.jenvman.2007.06.027.

Sasser, Charles E., Jenneke M. Visser, Edmond Mouton, Jeb Linscombe, and Steve B. Hartley. 2014. "Vegetation Types in Coastal Louisiana in 2013." *U.S. Geolgoical Survey Scientific Investigations Map 3290, 1 Sheet, Scale 1:550,000*, 3290. doi:http://dx.doi.org/10.3133/sim3290.

Steyer, Gregory D. 2010. "Coastwide Reference Monitoring System." *US Geological Survey Fact Sheet 2010-3018*, no. August.

Steyer, Gregory D., Brady R. Couvillion, and John A. Barras. 2013. "Monitoring Vegetation Response to Episodic Disturbance Events by Using Multitemporal Vegetation Indices." *Journal of Coastal Research* 63 (63): 118–30. doi:10.2112/SI63-007.1.

Tucker, Compton J. 1979. "Red and Photographic Infrared Linear Combinations for Monitoring Vegetation." *Remote Sensing of Environment* 8 (2): 127–50. doi:10.1016/0034-4257(79)90013-0.

Turner, R. Eugene. 1997. "Wetland Loss in the Northern Gulf of Mexico: Multiple Working Hypotheses." *Estuaries* 20 (1): 1–13. doi:10.2307/1352716.

"UAS Master Inpho Software." 2016. Trimble Navigation Limited. http://www.trimble.com/Geospatial/Inpho-UASMaster.aspx.

Yang, J., and F. J. Artigas. 2010. "Mapping Salt Marsh Vegetation by Integrating Hyperspectral and LiDAR Remote Sensing." In *Remote Sensing of Coastal Environments*, 173–90.